The impact of space weather on very low Earth orbit (VLEO) satellites

Vishal Ray
University of Colorado Boulder
Tom E. Berger
University of Colorado Boulder

Zach C. Waldron
University of Colorado Boulder

Eric K. Sutton
University of Colorado Boulder

Greg Lucas
University of Colorado Boulder

Delores J. Knipp
University of Colorado Boulder

Jeffrey P. Thayer
University of Colorado Boulder

Siamak G. Hesar
Kayhan Space Corp.

Daniel J. Scheeres
University of Colorado Boulder

1. INTRODUCTION

Shortly following the 36th launch of SpaceX's Starlink constellation on 3 February 2022, 38 out of 49 satellites were lost due to the impacts of a modest geomagnetic storm that reached G1 intensity earlier that day [1]. The satellites were placed into an initial orbit of 210 km after which they were intended to maneuver to an operational altitude of 500 km. While this low altitude plan lent itself to a quick de-orbit in the face of catastrophe, it exposed the satellites to the uncertainties in neutral density associated with relatively meager space weather conditions. This event has served as a reminder to the commercial space community for the need to better model and predict atmospheric drag, especially at these very high drag environments.

Recently, there's been a renewed interest in exploring the very low Earth orbits (VLEO) for sustained satellite operations and as parking orbits before raising the satellite to its operational altitude such as Starlink. With increasing congestion in Low Earth Orbit (LEO) and its associated collision risks, VLEO could provide an additional orbital regime where satellites could reap the benefits of the LEO regime, thereby reducing the burden on the LEO regime. There are multiple advantages to utilizing VLEO for satellite operations. First and foremost, are the obvious environmental advantages - in such low altitudes, the increased effect of atmospheric drag implies an easier and faster end-of-life deorbiting capability. For example, at 300 km, the satellite lifetime will be under a year, irrespective of the

space weather conditions and for reasonable values of the ballistic coefficient. There are payload advantages that are obtained at lower altitudes - the spatial resolution of an imaging instrument is considerably improved with decreasing altitude [2]. In terms of satellite communications, the free space loss reduces at a lower altitude leading to an increased signal to noise ratio [2]. The low altitudes can be beneficial for numerous scientific applications such as in the fields of geodesy (improved gravity field) and aeronomy (investigation of the upper atmosphere). For example, the Gravity Field and Steady-State Ocean Circulation Explorer (GOCE) satellite [3] was launched at around 250 km to provide an accurate mapping of Earth's gravity field. A near-continuous low thrust mechanism was used to compensate for the drag and sustain the orbit. A few system engineering studies have been carried out for VLEO satellite missions that discuss the technical requirements to be able to sustain an operational satellite at these low altitudes [4, 5].

Even with the various advantages that VLEO offers, there are significant technical challenges to overcome before a widespread use of VLEO can be achieved for satellite operations. The large effects of atmospheric drag also translate to an increased maneuver cost for orbit maintenance along with an increased atomic oxygen erosion of spacecraft materials. Additionally, the uncertainties of atmospheric density modeling can lead to hundreds of kilometers of prediction errors within a day. This is further exacerbated by the large variability of the thermosphere in response to space weather disturbances. The increased density can also result in large aerodynamic torques that the attitude control system has to compensate for. Therefore, the increased atmospheric drag serves as both a significant benefit and the primary challenge for VLEO operations. It is important to understand the current limitations of the atmospheric density modeling both in terms of nowcasts (for orbit determination) and forecasts (for orbit prediction and evaluating fuel margins for station-keeping).

Earth's upper atmosphere is driven by a broad range of external energy inputs, leading to complex thermal, electromagnetic, and chemical processes, that result in a thermospheric neutral mass density ρ that is highly dynamic and whose variability is difficult to specify [6]. This leads to atmospheric drag being the largest source of orbit uncertainty of LEO satellites [7]. With decreasing altitudes, even a relatively small uncertainty can cause large orbit determination and prediction errors due to the compounding effect of the drag force. There are two broad categories of atmospheric density models that are used in orbit determination - physics-based models and semi-empirical models. Physics-based models take the form of general circulation models which solve the first-principle equations that govern the coupled thermosphere-ionosphere system. These are computationally very expensive and therefore, not used in satellite operations. Semi-empirical models offer excellent climatological pictures of upper atmospheric variability and can be run quickly. The most prevalent of these in operational use are the Mass Spectrometer Incoherent Scatter radar (MSIS), Drag Temperature Model (DTM) and Jacchia-Bowman (JB) series of models. Though significant differences are seen in the density output of the models, it is not always clear which models performs the best in operational use. For example, the estimated uncertainty of NRLMSISE-00 densities is 15% and for JB2008, it is 10% under mean conditions. But for extreme conditions or short-term and local-scale variations, the uncertainties can go up to 100% [8]. With newer upgrades to these models such as NRLMSIS 2.0 [9] and DTM-2020 [10] available to the community, the densities seem to be in better agreement with each other. It is also evident from the upgrades that the older density models consistently underestimate the densities when compared to estimates from CHAMP, GRACE and GOCE [10], especially during geomagnetic storms. This discussion is meant to point out the serious lack of agreement in the density model outputs during perturbed space weather conditions.

In this work, we explore the impacts of disturbed space weather conditions on satellite mission planning and operations. Our goal is to point out the need to account for elevated satellite drag and significantly larger drag uncertainties when making design decisions for satellite missions. We discuss the nature of space weather disturbances in the context of NOAA's classification of space weather events and look at the space environment projected into the coming few years. This equips us to understand the space weather conditions and events that led to the loss of the Starlink satellites in February 2022. Next, we compare the impacts of a minor geomagnetic storm (the Starlink loss event) and a major geomagnetic storm (the 2003 Halloween storm [11]). Finally, we end with a call to the community to account for space weather uncertainties for satellite operations as we head towards increased solar activity in the next decade.

2. CLASSIFICATION OF SPACE WEATHER EVENTS

Our Sun undergoes a 11-year cycle called the solar cycle where the magnetic field of the Sun flips over, i.e., the north and the south poles interchange. During the solar cycle, the activity on the Sun's surface changes as well. As we head towards a solar maximum, where the sunspot number is expected to peak in July 2025, the frequency of violent

disruptions on the Sun's surface is going to increase [12]. This will lead to an increase in radiation flux and magnetic field from the Sun through Coronal Mass Ejections (CMEs) and Solar Energetic Particles (SEPs) in the coming decade. Bundles of ejected magnetic field link to Earth's geomagnetic field transferring energy into Earth's magnetosphere. Some of this energy is dissipated in Earth's upper atmosphere. These interactions will lead to an increase in the thermospheric density and consequently, the atmospheric drag acting on LEO satellites. There are different indices and proxies that are used as indicators of the solar and geomagnetic activity. The solar radiation flux at 10.7 cm wavelength, the so-called F10.7 index, is commonly used as an indicator of solar activity in atmospheric models. The increase in solar radiation flux heats up the Earth's atmosphere. This causes the atmosphere to expand to higher altitudes and consequently, the neutral densities at the upper atmosphere to increase. A similar mechanism plays out for the particle flux from the Sun. The ejected particles arriving on Earth interact with the Earth's magnetic field and precipitate into the upper atmosphere. Their interaction with the atmospheric particles causes frictional heating and increase in the densities. Electric currents that form when the solar magnetic field bundles link with Earth's magnetic field also dissipate heat in the thermosphere, which adds to atmospheric density variations. The three-hour Ap and Kp indices are commonly used as indicators of the geomagnetic activity.

NOAA classifies the geomagnetic storms based on geomagnetic indices and the expected impacts on Earth. Fig. 1 describes the classification of geomagnetic storms, their impacts on spacecraft operations and their average frequency. Even though the average frequency for extreme geomagnetic storms is relatively low (4 days per 11 years), a single event can cause serious disruptions of spacecraft operations in LEO. Berger et al. [13] note that during the 2003 Halloween storm that reached extreme (G5) storm levels, "anecdotal testimony from USAF operators during the storm recounts that the majority of LEO satellites were temporarily lost, requiring several days of around-the-clock work to reestablish the catalog." They also show that even a moderate storm can have significant effects on the orbit propagation error, especially for satellites with perigees at VLEO altitudes. Along with increased positional uncertainty, there's a significant increase in fuel required for station-keeping and control torques for attitude stabilization as will be seen in the next few sections.

Scale	Description	Effect on spacecraft	Physical measure	Average frequency (1 cycle = 11 years)
G5	**Extreme**	May experience extensive surface charging, problems with orientation, uplink/downlink and tracking satellites.	Kp = 9 (Ap = 400)	4 days per cycle
G4	Severe	May experience surface charging and tracking problems, corrections may be needed for orientation problems.	Kp = 8, including a 9- (Ap = 179 to 300)	60 days per cycle
G3	Strong	Surface charging may occur on satellite components, drag may increase on low-Earth-orbit satellites, and corrections may be needed for orientation problems.	Kp = 7 (Ap = 111 to 154)	130 days per cycle
G2	Moderate	Corrective actions to orientation may be required by ground control; possible changes in drag affect orbit predictions.	Kp = 6 (Ap = 67 to 94)	360 days per cycle
G1	Minor	Minor impact on satellite operations possible.	Kp = 5 (Ap = 39 to 56)	900 days per cycle
G0	Nominal/Quiescent	Nominal conditions for spacecraft operations	Kp < 5 (Ap < 32)	

.

Fig. 1: Classification of geomagnetic storms by NOAA

3. FEBRUARY 2022 STARLINK LOSS EVENT

The 49 Starlink satellites launched at 18:13 UT on 03 February 2022 already had it worse compared to all the previous launches. As shown by the time-series of the Ap and F10.7 indices in Fig. 2, a minor geomagnetic storm of G1 intensity was in progress during the launch. The atmospheric density was 50 % higher than previous launches. The Ap index reached a peak of 56 at 09:00 UT and had recovered to 15 during the Starlink launch. But since there's a delay between the peak in the geomagnetic storm and the response of the thermosphere to the forcing due to thermal inertia, the peak of the atmospheric density almost coincided with the Starlink launch. As the thermosphere recovered, a second G1 geomagnetic storm hit, reaching a peak of Ap = 56 at 15:00 UT on 04 Feb. The atmospheric density modeled by HASDM reached a peak 8 hours later and showed an increase of 28 % compared to the nominal density averaged over the past 9 days as shown in Fig. 3. The thermosphere had not yet recovered when the second storm commenced, which explains the further increase in density though the storm magnitudes were similar in terms of the planetary Ap index. The Starlink satellites reentered the Earth's atmosphere on 07 Feb. It is noteworthy that the official pre-launch forecasts and nowcasts of space weather conditions were limited to solar flare activity which provided no warning of the ongoing (or incoming) geomagnetic storm impacts to the LEO environment.

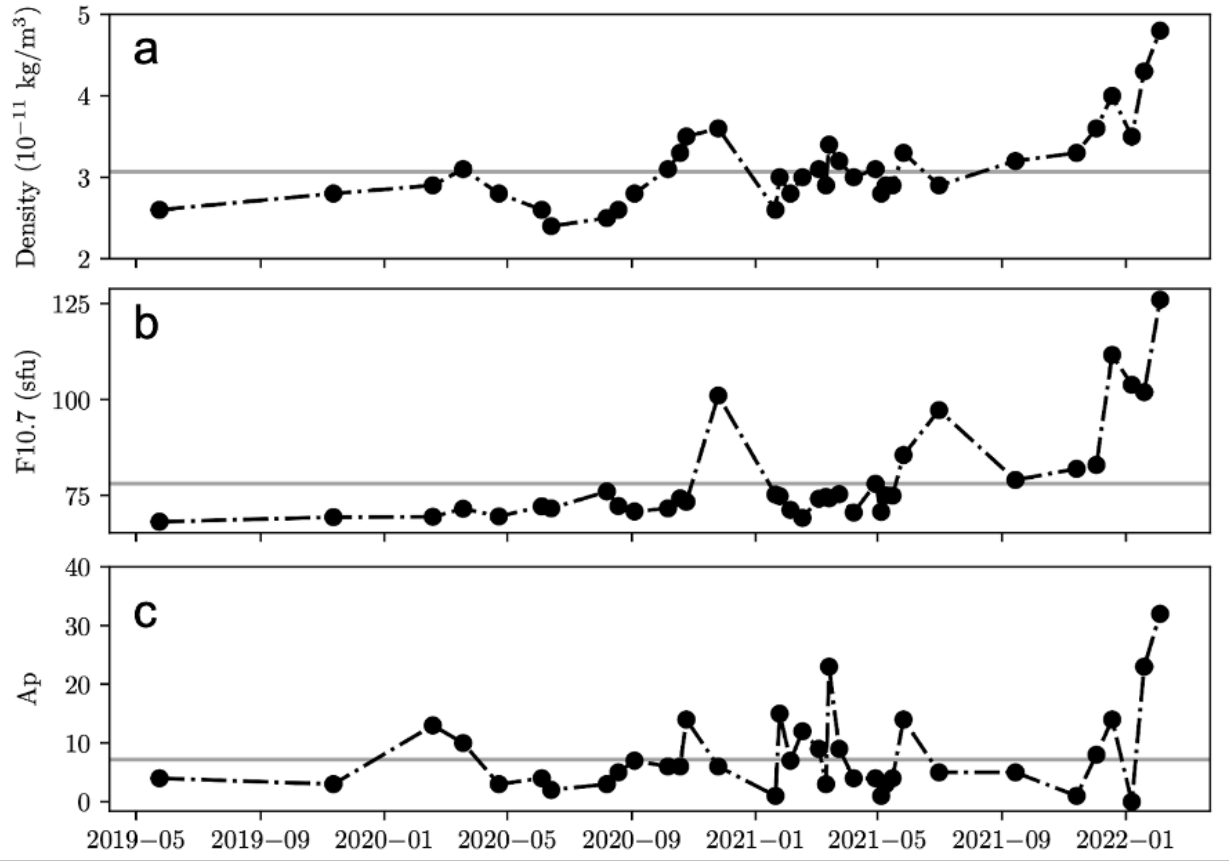

.

Fig. 2: (a) Orbit averaged thermospheric density derived from the NRLMSIS2.0 model [9]; (b) Solar F10.7cm radio flux in Solar Flux Units (sfu; 1 sfu = $10^{-22} W m^{-2} Hz^{-1}$) ; and (c) the planetary geomagnetic Ap index for prior 35 Starlink launches leading up to the loss event on 03–04 February 2022. The grey line in each panel denotes the average value over the entire series. The density data show that relative to the earlier Starlink launches in 2022, thermospheric density during the 03 Feb 2022 launch was approximately 50 % higher than the average for previous launches.

The drag environment experienced by the Starlink satellites at the parking altitude can be mapped by analyzing the tracking data. The GPS-derived positions and velocities as well as the attitude information for one of the Starlink

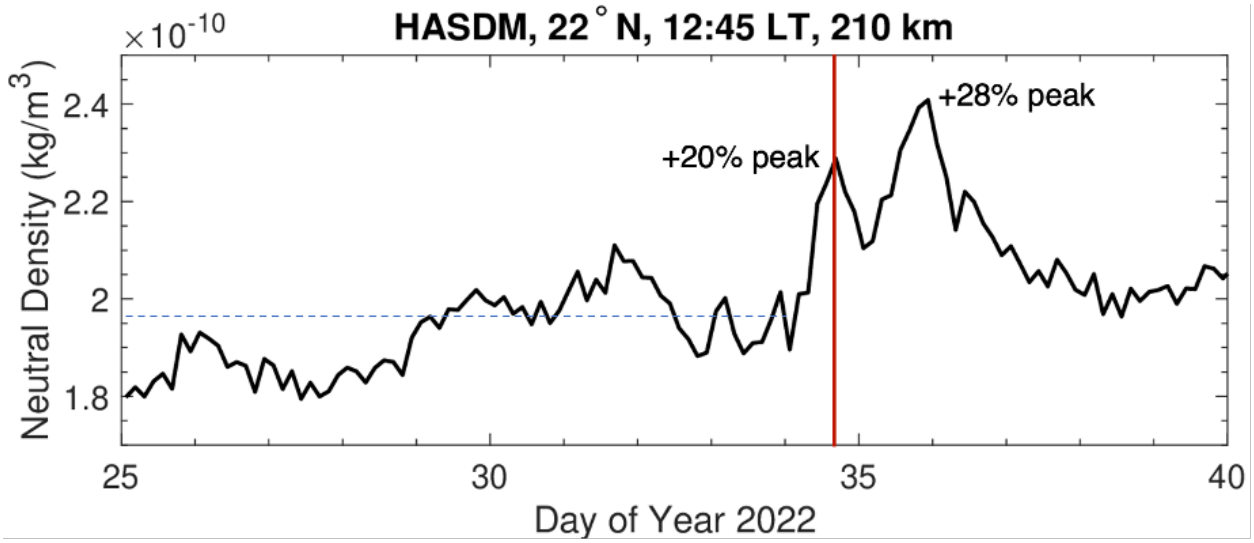

.

Fig. 3: Thermospheric neutral density values inferred from the HASDM model at 210 km altitude, 22° N Latitude, and 12:45 Local Time (LT) for DOY 25 to 45, 2022 (25 Jan. – 14 Feb. 2022). The latitude and LT values were taken from Two Line Element (TLE) data for one of the Starlink satellites tracked before re-entry. The launch and anomaly occurred on the evening of 03 Feb (DOY 34, vertical red line), just as inferred density values peaked due to the first G1 geomagnetic storm. Approximate average density value over the 9 days prior to the launch against which the peak density values are compared is indicated by the blue dashed line. The main re-entry event occurred on DOY 38 (07 Feb).

satellites from the Feb 2022 launch are available. The tracking data are fed as measurements into an orbit determination method framework. A high-fidelity force model is used for the orbit propagation in the filter with a 120x120 gravity field, third-body forces of Sun and Moon, box-wing solar radiation pressure, solid Earth and ocean tides, atmospheric drag and lift/side forces. The atmospheric density is estimated from the tracking data using a stochastic process model in a "POD accelerometry" scheme, e.g., [14]. A physics-based model of the drag-coefficient is used to extract the densities. At such low altitudes, the reflection of the gas molecules from the satellite surface is usually assumed to be diffuse with nearly complete accommodation. This is because the satellite surface becomes rough the longer it stays in orbit due to the adsorption of atomic oxygen on the satellite surface. But the data we have for the Starlink satellites corresponds to a few days immediately following orbit insertion. Due to the smaller amount of time spent in orbit, it is possible that the reflection pattern is closer to clean rather than rough surfaces. Laboratory experiments performed on clean surfaces suggest a more specular reflection of the gas molecules [15]. The drag-coefficients for diffuse and specular reflection are plotted in Fig. 4. It is interesting that the diffuse drag-coefficient is significantly larger than the usual cannonball value of 2.2 due to the large solar panels tangential to the flow as seen in Fig. 4. The relatively large tangential drag contributes to an increased drag-coefficient as is commonly seen in slender shaped satellites such as GOCE [16]. The uncertainty in the drag-coefficient introduces a large uncertainty in the density.

The POD-estimated densities near the perigee are compared with JB2008, NRLMSIS2.0 and HASDM modeled densities in Fig. 5. It is evident that the purely diffuse drag-coefficient vastly underestimates the density while the purely specular drag-coefficient overestimates the density. This seems to indicate that the nature of the reflection is quasi-specular and will lie somewhere in between the two extremes.

The atmospheric densities near the perigee are elevated before Feb 2022 due to the storm. But is is clear from Fig. 5 and the HASDM densities in Fig. 3 that the increase in densities was not very significant though it still lead to unfortunate consequences. The effect of this minor storm on operations serves as a warning call to prepare for satellite operations during more severe geomagnetic storms that we may experience in the next decade as we head towards a solar maxima.

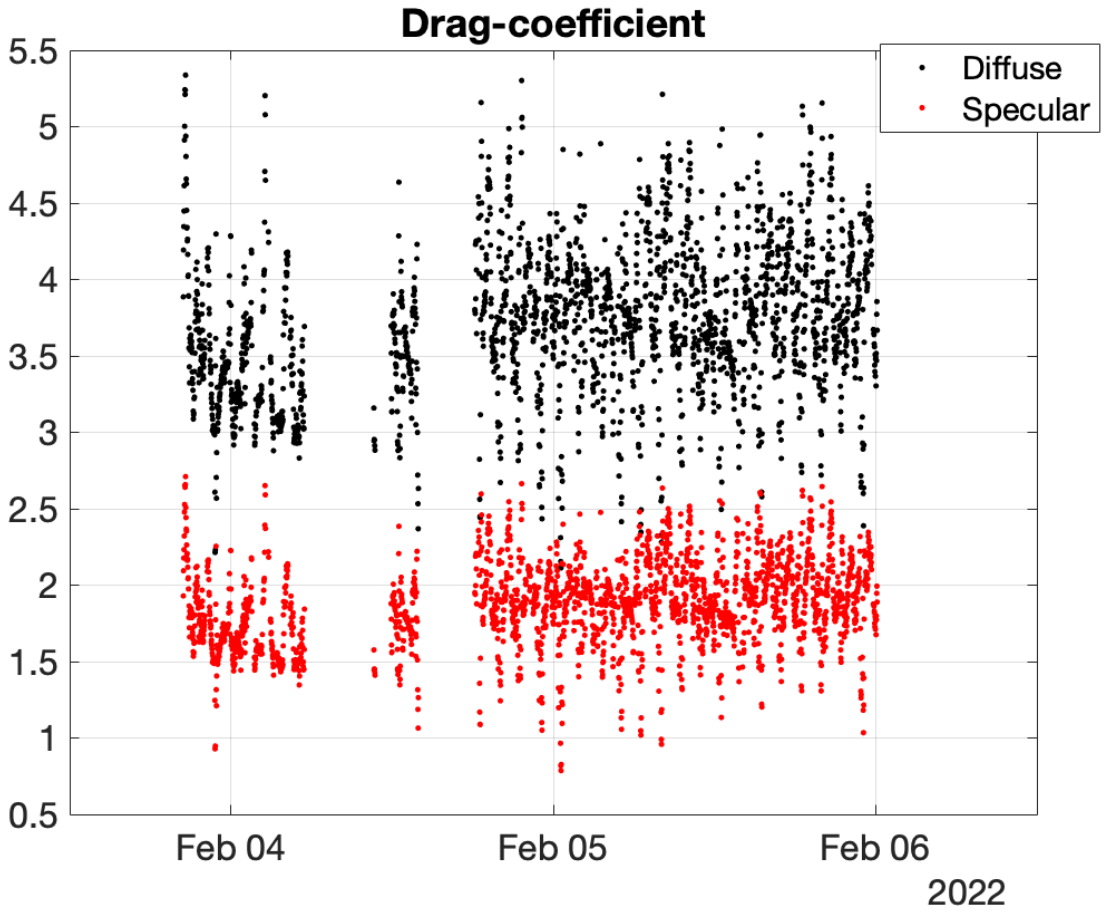

Fig. 4: Drag-coefficient for the Starlink satellite during Feb 3-5, 2022. Note that the high values are due to the large tangential drag experienced in the open-book configuration.

4. ORBITAL IMPACTS DURING GEOMAGNETIC STORMS

As shown in the previous section, the maximum density increase at 200 km altitude due to the G1 storms of February 2022 was only about 20–30 %. The Starlink satellite loss illustrates that even this relatively minor density increase was consequential due to a lack of forecast. However we know that in severe and extreme geomagnetic storms, thermospheric neutral density can increase significantly, sometimes by orders of magnitudes at higher altitudes. It is therefore of interest to examine what the impact of an extreme G5 geomagnetic storm would be on the Starlink satellites at both their staging altitudes of 200–300 km and the operational altitude of 550 km. In addition, it is important to note that all satellites and debris objects in LEO will be impacted by thermospheric density increases during extreme geomagnetic storms. To better prepare for severe geomagnetic storm impacts on satellite operations and mission planning, it is imperative to understand the potential impacts on satellite trajectories at all altitudes.

To illustrate the expected impacts of an extreme storm relative to a minor one, sample equatorial LEO satellites are propagated in orbits of various altitudes (210 km, 250 km, 350 km and 550 km) for two geomagnetic storm conditions: a G5 level storm replicated from the 29 Oct. 2003 storm (the “2003 Halloween storm”), and a G1 level storm replicated from the 02 Feb., 2022 storm that caused the Starlink loss event. A “Starlink-type” geometry and mass specification with an “open-book” configuration (minimum-drag) is assumed for the sample satellite. The altitude decay is plotted for a similar orbit as the Starlink satellites with perigee at 210 km and apogee at 340 km, during 4-day duration G1 and G5 geomagnetic storms in Figure 7. HASDM is used as the reference density model. The figure also shows

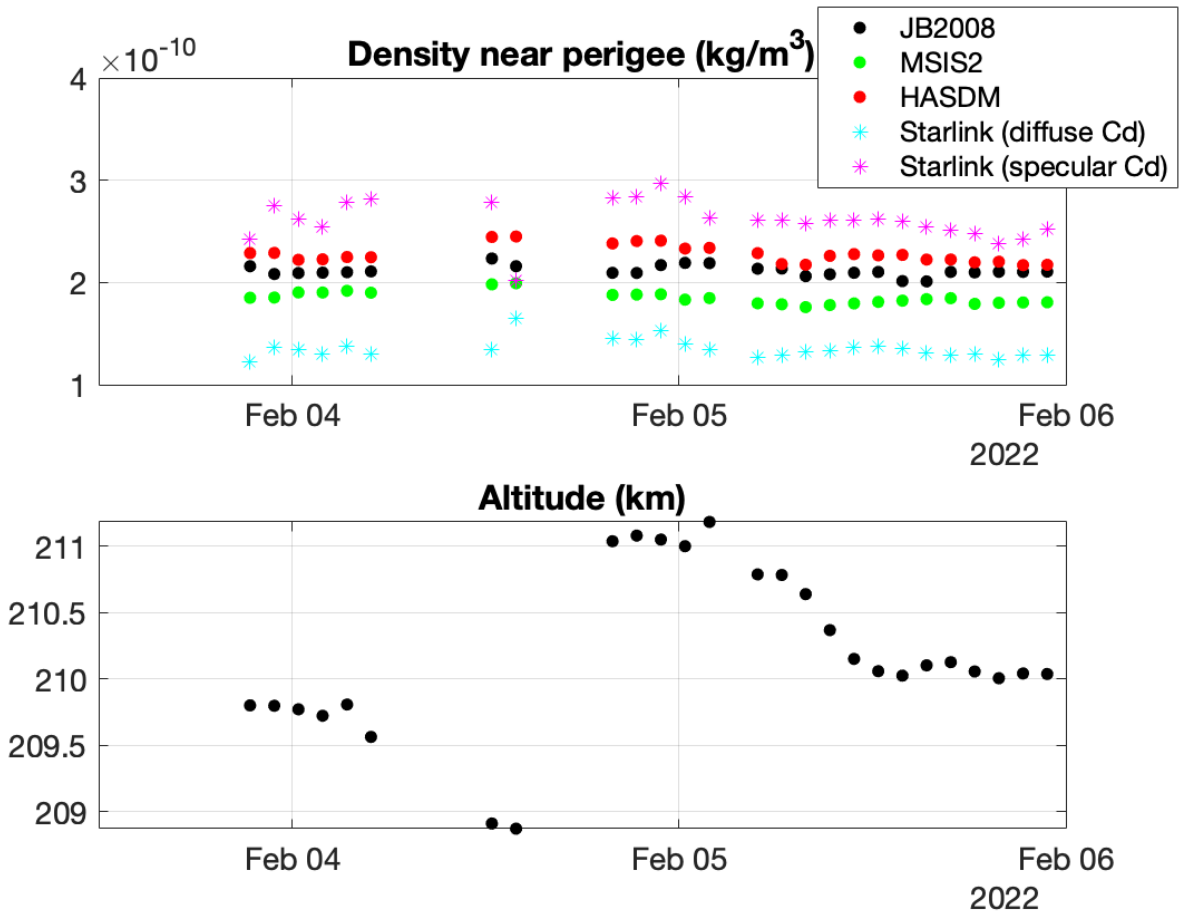

Fig. 5: (a) Atmospheric densities near the perigee estimated from the Starlink tracking data and attitude information and modeled using JB2008 and NRLMSIS2.0 during the Feb 3-4, 2022 period. (b) Corresponding altitude of the satellite near the perigee

the corresponding changes in the in-track position relative to a reference orbit unperturbed by atmospheric drag. The in-track position (δs) is calculated along the curved path of the satellite as follows [17]

$$\delta s = \delta M(v(t))/(n(t)) \tag{1}$$

where δM is the change in Mean anomaly, $v(t)$ is the speed of the satellite, $n(t)$ is the mean motion of the satellite. The altitude decay of a Starlink-like satellite at 210 km perigee altitude ranges from 20 km over 5 days for the G1-level storm to around double the amount for the G5 storm over the same duration. The change in the in-track position is around 60 % more for a G5 storm compared to a G1 storm.

The varied orbital changes during different storm periods is an important factor for consideration when planning for station-keeping and collision avoidance. This requires predicting the satellite orbits into the future using a given atmospheric density model. Depending on the model used, the orbit prediction can vary significantly. Figure 8 shows the in-track error incurred for the same storms for the JB08 and MSISE-00 models relative to HASDM at two higher altitudes. The in-track error at 250 km altitude is between 180 km (JB08) and 250 km (MSISE-00) over the G5 storm duration. At 350 km altitude, the in-track error is between 40 km (MSISE-00) and 50 km (JB08) over the storm duration. The error decreases to between 1.5-2 km at 550 km due to the much lower absolute mass densities at that altitude as shown in Fig. 6. The differences in model results are driven primarily by the well-known fact that the accuracy of semi-empirical density models is significantly diminished during severe geomagnetic storms [18]. Moreover, depending on the severity of the geomagnetic storm, the density models can evidently under-predict or

over-predict the densities (and hence drag forces and in-track errors) relative to one another. This is evident from the difference in signs of the in-track error for MSISE-00 for the two storm periods. The HASDM assimilative model uses the JB08 model as its base state model so the differences shown between those models directly illustrates the reductions in altitude and in-track error enabled by data assimilation. Orbital velocities at that altitude are 7–10 km/s so this level of in-track error represents less than one-second of satellite travel time and may not impact communications significantly. But conjunctions estimates can be severely affected by the increased uncertainty around the position estimates introduced by the density model used. The purpose of these simulations is to point out the importance of accurate density forecasts for constrained orbit predictions rather than commenting on the accuracy of specific models.

One important consideration here is the sensitivity of the orbital impacts to the ballistic coefficient. In these simulations, the ballistic coefficient is considered to be constant at the minimum drag configuration. But in reality, there can be strong torques acting on the satellite that the attitude control system (ACS) may not be able to handle. The satellite could possibly deviate from its nominal attitude and even start detumbling. In such a case, the experienced orbital impacts might be greatly increased, depending on the frontal cross-sectional area. This is especially true for satellites such as Starlink, whose ballistic coefficient can vary by an order of magnitude between the minimum and maximum drag configurations. For example, the satellite will reenter within a few hours during either of the storms at the Starlink parking orbit altitude, 210 km, for the "shark-fin" configuration, i.e., solar panels perpendicular to the flow. With a larger ballistic coefficient, the orbit is also more sensitive to changes in the density. Therefore, the differences between the two storm periods will be amplified for a larger ballistic coefficient.

It is important to note that even for satellites with on-board GNSS receivers, ionospheric disturbances during extreme geomagnetic storms can lead to loss of lock over significant portions of the orbit [19], particularly for polar orbiting satellites at lower LEO altitudes. Thus GNSS-derived satellite states may be unavailable or inaccurate during severe geomagnetic storms and operators will need to rely on high-fidelity orbit propagation models to prevent loss of tracking events. During extreme events, loss of tracking can lead to downlink and uplink communication disruption as ground antennas fail to acquire satellites that are potentially hundreds or thousands of km off-track, ultimately requiring time-consuming radar re-acquisition exercises by military or commercial networks.

5. ASSESSMENT OF FUEL REQUIREMENTS FOR STATION-KEEPING

It is clear that the orbital impacts can be drastically different for varying geomagnetic storm intensities. At lower altitudes, relatively small variations in the density can lead to much larger changes in the orbit states due to the high drag environment. It is important to account for the possible variations in the drag force due to perturbed space weather conditions during the mission design phase, especially when deciding the onboard fuel requirements for orbit raising, station-keeping etc. In this section, we carry out an analysis of how station-keeping fuel requirements would change for different geomagnetic activities, ignoring any potential drag-force changes due to attitude.

A preliminary estimate of the total delta-v required for station-keeping of a satellite subject to satellite drag over some time duration can be obtained by integrating the drag acceleration. This is equivalent to assuming a continuous thrust-drag cancellation, such that the satellite experiences zero drag force and consequently, zero change in the orbital elements due to drag. This strategy is implemented by some scientific missions to null out uncertainties introduced in the satellite states for the purpose of precise science measurements, such as for precise gravity mapping by GOCE [20]. Future missions for gravitational wave detection such as the Laser Interferometry Space Antenna (LISA) [21] and Deci-hertz Interferometer Gravitational wave Observatory (DECIGO) [22] will use advanced drag-free cancellation technologies to ensure pure free fall of the satellite.

The delta-v required to continuously cancel out the drag force for one complete day is plotted in Fig. 8 for satellites in circular orbits at the altitudes of 200-400 km during the G1 and G5 geomagnetic storms described in the previous section. The Starlink open-book configuration is considered as the representative configuration with an average area-to-mass ratio (AMR) of 0.005, which is on the lower end of AMRs. The results can be scaled up or down, depending on the AMR. It is evident that there's a significant increase in the fuel required during a G5 geomagnetic storm compared to a G1 geomagnetic storm. At 200 km, about 50 % more fuel is required during a G5 geomagnetic storm. The number steadily increases for higher altitudes though the effects at higher altitudes are less important since the density, and therefore, the thrust required is smaller. If the maneuvers are instead performed depending on some threshold on the altitude decay, the frequency of the maneuvers will be higher during an extreme geomagnetic storm. On the other hand, if the maneuvers are performed after a fixed duration, recovery to the nominal orbit will be much more difficult

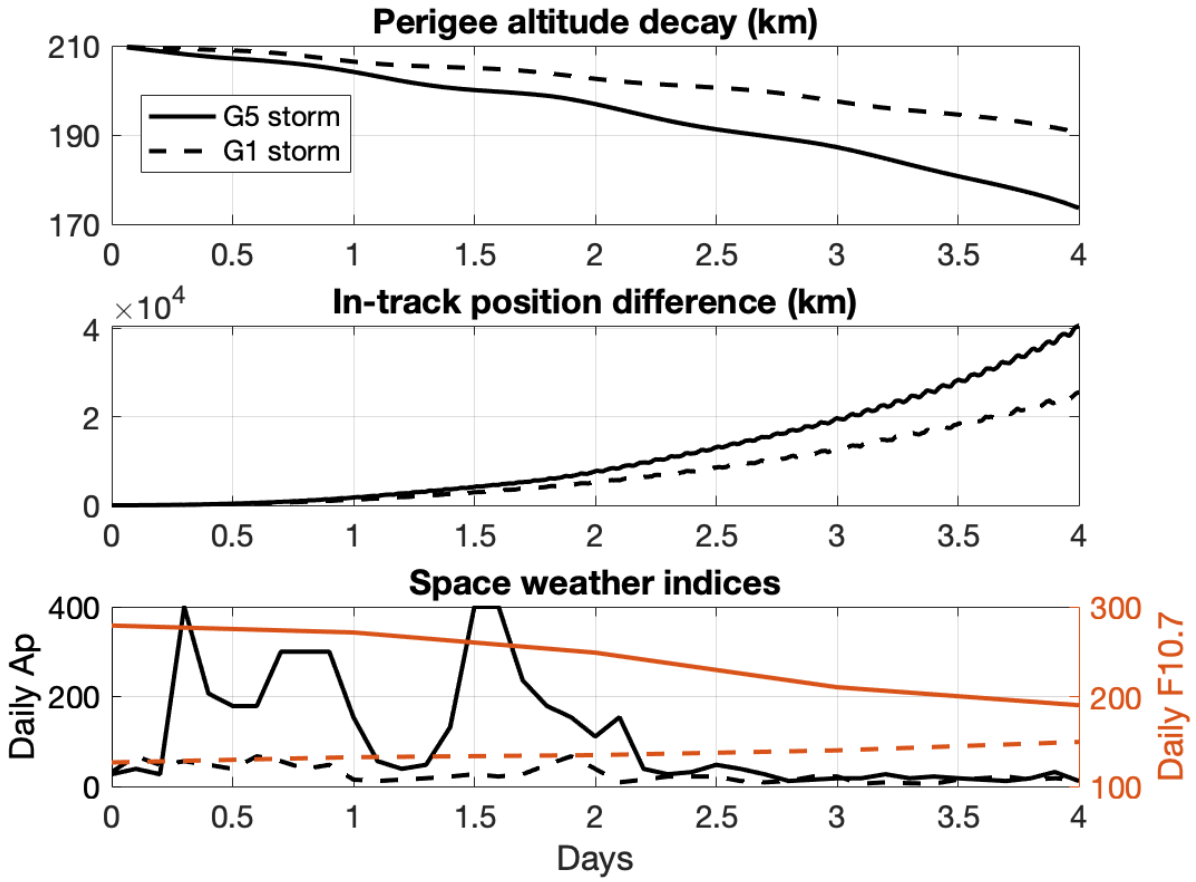

Fig. 6: (a) Perigee altitude decay and (b) change in the in-track position relative to an orbit unperturbed by atmospheric drag for a 'Starlink-type' satellite with a fixed attitude to produce minimum drag force in an eccentric orbit with the perigee altitude at 210 km and apogee altitude at 340 km orbit during a G1 and G5 geomagnetic storm. (c) Planetary geomagnetic Ap index and F10.7 radio flux in solar flux units for the simulated G1 and G5 storms. The solid lines show a representative extreme G5 geomagnetic storm (the "Halloween 2003" storm) and the dashed lines show synthetic data considered during the 03 Feb 2022 G1 geomagnetic storm.

during an extreme geomagnetic storm.

The low-thrust propulsion systems used for thrust-drag cancellation have limitations on the maximum thrust that they can generate. If the drag force is larger than the maximum thrust, the thruster will not be able to wholly compensate for the drag. This is a possible scenario during extreme geomagnetic storms where the instantaneous drag force can increase by orders of magnitude. In such cases, the orbit will continue to decay due to the residual drag force until the storm subsides. The time-series of the drag-force acting on the Starlink-type satellite during the two storm scenarios is plotted in Fig. 9. For context, current ion thrusters can produce around 50-250 mN of maximum thrust with laboratory tests producing up to a few Newtons of thrust [23] - higher the thrust, heavier the propulsion system. Moreover, the drag force can be significantly larger for a different AMR. For example, the force acting on the Starlink satellites can increase by an order of magnitude when the satellite is in a Shark-fin configuration, i.e., the solar panel is perpendicular to the bus. Therefore, during extreme storm periods, it is quite probable for the propulsion system to be unable to compensate for the drag force and consequently, for the satellite to experience significant orbital disruptions. Additionally, as discussed earlier, the effects of the potential attitude control loss during storm periods are coupled with the propulsion system required to maintain the orbit. Since thrusters are highly directional, any deviations from the nominal attitude can lead to a loss of efficiency in orbit maintenance. In fact, for large deviations, the thrusters

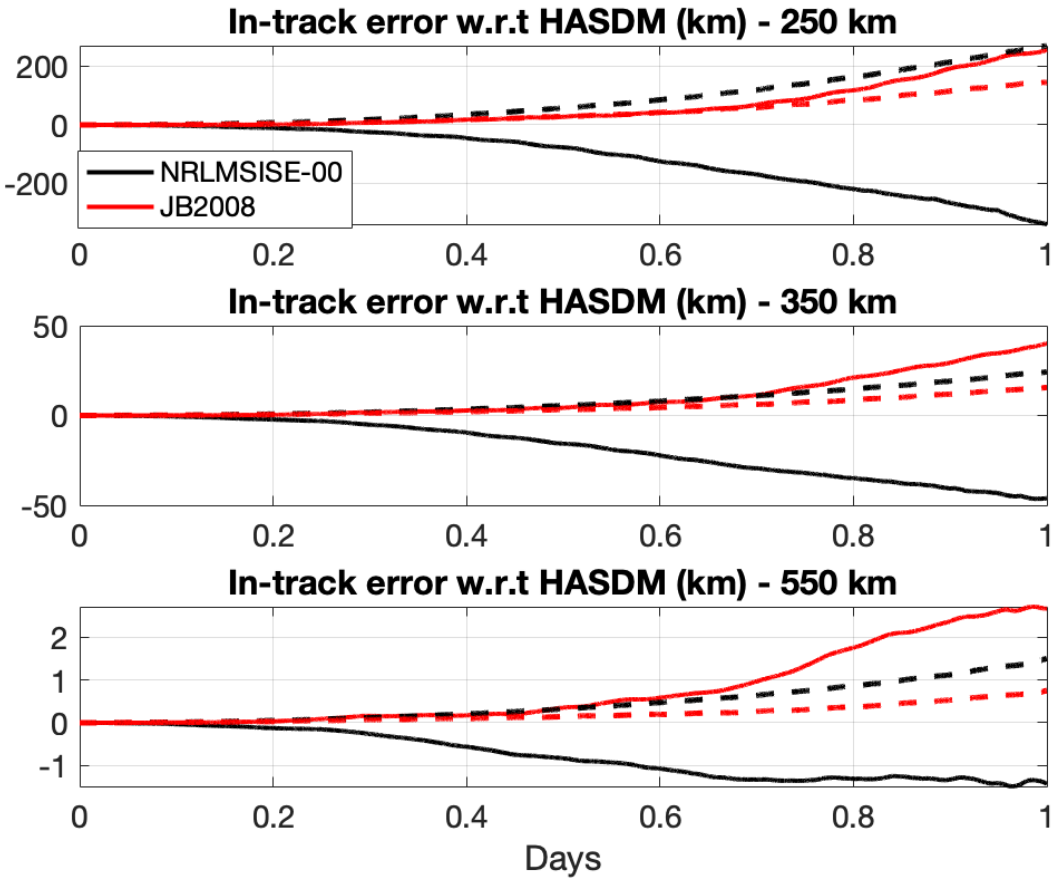

.

Fig. 7: (a) In-track positional error incurred over one day when using the MSISE-00 or JB08 models with respect to HASDM as the reference density model during G1 and G5 geomagnetic storms for a 'Starlink-type' satellite at (a) 250 km; (b) 350 km; and (c) at 550 km . The solid lines show results for a G5 geomagnetic storm and the dashed lines show results for a G1 geomagnetic storm. Note that the underlying thermosphere model for HASDM is the JB08 model; the curves for JB08 error relative to HASDM shown above thus reflect the correction of JB08 errors due to data assimilation at any storm level. The errors at 250 km for both models at either storm level are an order of magnitude larger than those at 350 km and two orders of magnitude larger than 550 km.

might be rendered temporarily useless. Therefore, a six degree of freedom analysis should be carried out for extreme storm periods during the mission design stage.

6. A CALL TO THE COMMUNITY

The Starlink loss event serves as a stark reminder that forecasting of the drag environment is crucial for making key mission decisions for satellites in VLEO altitudes. As discussed here, the density increase due to the minor storm, classified as G1 by NOAA, would not have been as concerning at higher altitudes. But at VLEOs, due to the high drag environment, orbital operations are more sensitive to changes in the density. In addition, multiple events can cascade quickly at these altitudes, leading to disastrous consequences. The orbital impacts of storm periods are highly coupled with the attitude control system. Any deviations from the nominal attitude, due to the satellite experiencing increased aerodynamic torques, can lead to large changes in the ballistic coefficient as well as loss of efficiency of the thrusters at best, and complete loss of use at worst. This, in turn, increases the rate of orbital decay. It can be quite difficult to recover from this compounding situation as the orbital decay leads to a continuous increase in the

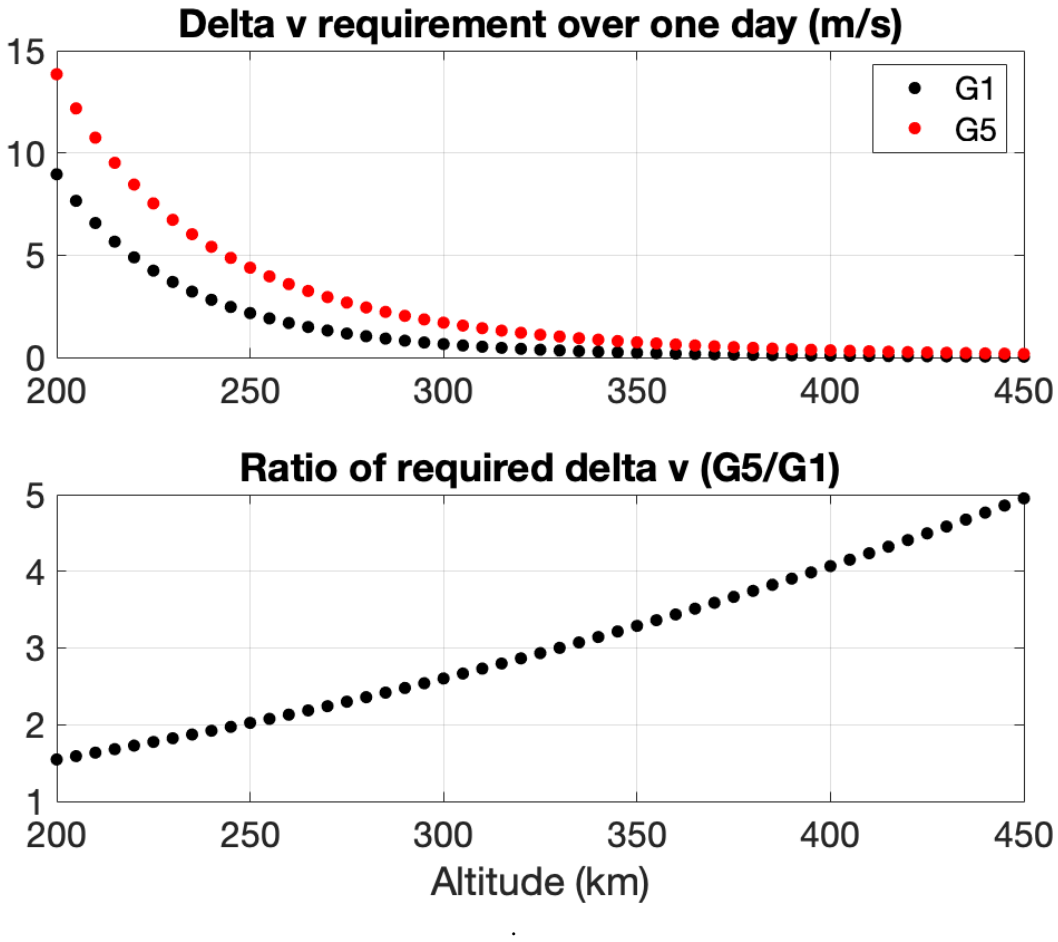

Fig. 8: (a) Total delta-v required over a day for continuous drag compensation during G1 and G5 geomagnetic storms. (b) The ratio of the required delta v during the G5 storm over the delta v required during the G1 storm. The plots are for an AMR of 0.005 which corresponds to the Starlink open-book configuration. The results can be scaled up or down, depending on the AMR.

drag. A similar situation might have occurred for the Starlink satellites as they were commanded into safe mode (the open-book configuration) to minimize atmospheric drag. But due to the increased drag torques, the satellites couldn't leave the safe mode to begin orbit-raising maneuvers [24]. This led to a quicker orbital decay than it would have been in quiescent conditions. Another historical event that brings the discussion to focus is the loss of attitude control for the International Space Station (ISS) in December, 2006. During a solar storm in December 2006, the Control Moment Gyroscopes (CMGs) onboard the ISS reached saturation, with one of the contributing factors being excessive atmospheric drag. But there were several other factors such as complex construction projects, equipment malfunction, and balky solar panels that had already made operations challenging [25]. The increase in atmospheric drag due to the solar storm served as the last straw in this cascading chain of events.

With the growing interest in the VLEO altitudes, it is important to consider the possibility of severe to extreme geomagnetic storms while analyzing orbital operations including tracking, station-keeping and attitude maintenance. Forecasting thermospheric neutral density perturbations that lead to higher satellite drag is complicated by the fact that the perturbations occur 10s of hours to several days after the root-cause solar magnetic eruption that generates the associated flare and Earth-directed Coronal Mass Ejection (CME). An accurate and reliable forecast of thermospheric neutral density during geomagnetic storms therefore requires a linked chain of models from the Sun to the upper atmosphere of the Earth. In particular, it requires a full-physics model of the ionosphere-thermosphere-mesosphere (ITM) system coupled on the lower boundary to a tropospheric and stratospheric general circulation model and on

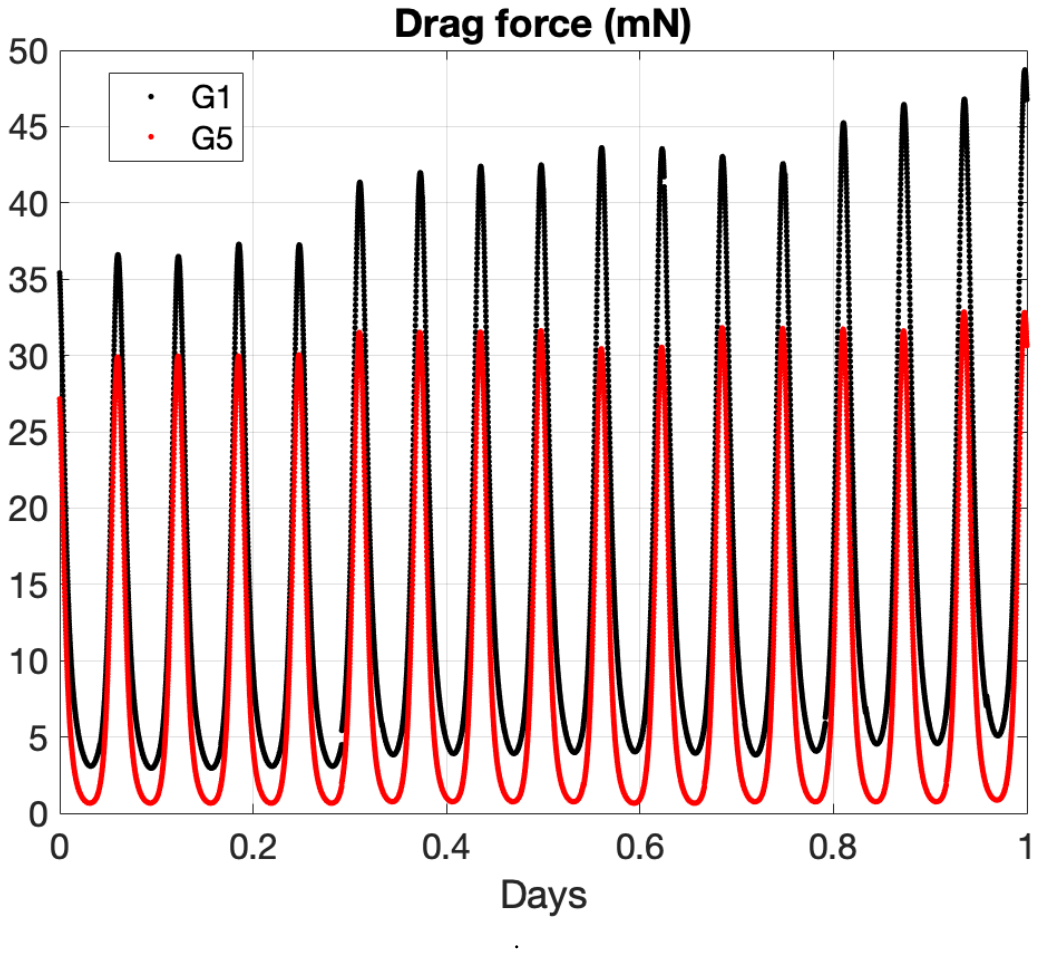

Fig. 9: The drag force acting on a Starlink-type satellite with an AMR of 0.005 during a G1 and G5 geomagnetic storms. The perigee is 210 km and apogee is 350 km.

the upper boundary to a full-physics model of the magnetosphere and plasmasphere, the regions of the Earth system which process the CME energy and plasma inputs. Development of this complex coupled model system is a goal of applied space weather research, but a fully-coupled operational space weather forecast model for the orbital space environment is still some years away.

In the meantime, a system of near real-time (NRT) measurements of thermospheric neutral density could provide launch and satellite operators with valuable "nowcast" information on conditions in LEO during geomagnetic storms. This could take a data-assimilation form that corrects for a baseline density model using real-time tracking from orbiting satellites - similar to the Air Force High Accuracy Satellite Drag Model (HASDM) [26] but available to non-military users. Such a system, had it been in place during the 03 February 2022 Starlink launch, could have warned Starlink operators that thermospheric neutral density at the 210 km staging altitude was significantly elevated relative to prior launches and allowed them to alter the launch time or staging altitude.

7. ACKNOWLEDGEMENTS

We are grateful to Dr. David Goldstein, Principal Guidance, Navigation and Control Engineer, SpaceX, for providing us the tracking data and attitude information for the Starlink satellites during the period of Feb 3-8, 2022. This material is based upon work supported by the National Aeronautics and Space Administration under Grant 80NSSC21K1554 issued through the Heliophysics Division Space Weather Science Application initiative, and Air Force STTR Phase 2

award No. FA864921P1517 in collaboration with Kayhan Space. Delores J. Knipp was partially supported by NASA Grant 80NSSC20K0199.

8. REFERENCES

[1] Mike Hapgood, Huixin Liu, and Noé Lugaz. SpaceX – sailing close to the space weather? *Space Weather*, 2022.

[2] N.H. Crisp, P.C.E. Roberts, S. Livadiotti, V.T.A. Oiko, C. Huyton, L.A. Sinpetru, K.L. Smith, S.D. Worall, J. Becedas, R.M. Domínguez, D. González, V. Hanessian, A. Mølgaard, J. Nielsen, M. Bisgaard, Y.-A. Chan, S. Fasoulas, G.H. Herdrich, F. Romano, C. Traub, D. García-Almiñana, S. Rodríguez-Donaire, M. Sureda, D. Kataria, R. Outlaw, B. Belkouchi, A. Conte, J.S. Perez, R. Villain, B. Heiberer, and A. Schwalber. The benefits of very low earth orbit for earth observation missions. *Progress in Aerospace Sciences*, 117, 2020.

[3] M.R. Drinkwater, R. Haagmans, D. Muzi, A. Popescu, R. Floberghagen, M. Kern, and M. Fehringer. The GOCE gravity mission: ESA'S first core earth explorer. In *3rd International GOCE User Workshop*, pages 1–7, 2007.

[4] N.H. Crisp, P.C.E. Roberts, F. Romano, K.L. Smith, V.T.A. Oiko, V. Sulliotti-Linner, V. Hanessian, G.H. Herdrich, D. García-Almiñana, D. Kataria, and S. Seminari. System modelling of very low Earth orbit satellites for Earth observation. *Acta Astronautica*, 187:475–491, 2021.

[5] Lance McCreary. A satellite mission concept for high drag environments. *Aerospace Science and Technology*, 92:972–989, 2019.

[6] J. T. Emmert. Thermospheric mass density: A review. *Advances in Space Research*, 56(5):773–824, 2015.

[7] M.D. Hejduk and D.E. Snow. The Effect of Neutral Density Estimation Errors on Satellite Conjunction Serious Event Rates. *Space Weather*, 16(7):849–869, 2018.

[8] ISO/FDIS 14222. Space environment(natural and artificial)- Earth upper atmosphere. International Standard, 2013.

[9] J.T Emmert, Drob D.P., J.M. Picone, D.E. Siskind, M. Jones Jr., M.G. Mlynczak, P.F. Bernath, E. Chu X, Doornbos, Funke B., L.P. Goncharenko, M.E. Hervig, M.J. Schwartz, P.E. Sheese, F. Vargas, B.P. Williams, and T. Yuan. NRLMSIS 2.0: A whole-atmosphere empirical model of temperature and neutral species densities. *Earth and Space Science*, 8(3), 2020.

[10] S. Bruinsma and C. Boniface. The operational and research DTM-2020 thermosphere models. *J. Space Weather Space Clim.*, 11(47), 2021.

[11] Tony Phillips. The day Earth lost half its satellites (Halloween Storms 2003). October 28, 2021.

[12] NOAA Weather Service. Hello SOlar Cycle 2025. September 15, 2020.

[13] T.E. Berger, M.J. Holzinger, E.K. Sutton, and J.P. Thayer. Flying through Uncertainty. *Space Weather*, 18, 2020.

[14] Vishal Ray, Daniel J. Scheeres, Suood Alnaqbi, W. Kent Tobiska, and Siamak G. Hesar. A Framework to Estimate Local Atmospheric Densities With Reduced Drag-Coefficient Biases. *Space Weather*, 20(3), 2022.

[15] I.K. Harrison and J.J. Swinerd. A free molecule aerodynamic investigation using multiple satellite analysis. *Planetary and space science*, 44(2):171–180, 1996.

[16] Vishal Ray, Daniel J. Scheeres, Suood Alnaqbi, W. Kent Tobiska, and Siamak G. Hesar. Satellite drag coefficient modeling for thermosphere science and mission operations. *Advances in Space Research*, 2022.

[17] J. T. Emmert, H.P. Warren, A.M. Segerman, J.M. Byers, and J.M. Picone. Propagation of atmospheric density errors to satellite orbits. *Advances in Space Research*, 59:147–165, 2017.

[18] Denny M. Oliveira, Zesta Eftyhia, Piyush M. Mehta, Richard J. Licata, Marcin D. Pilinski, Kent W. Tobiska, and Hisashi Hayakawa. The Current State and Future Directions of Modeling Thermosphere Density Enhancements During Extreme Magnetic Storms . *Frontiers in Astronomy and Space Sciences*, 8, 2021.

[19] Shixuan Zhang, Liming He, and Lixin Wu. Statistical Study of Loss of GPS Signals Caused by Severe and Great Geomagnetic Storms. *JGR Space Physics*, 125(9), 2020.

[20] Enrico Canuto. Drag-free and attitude control for the GOCE satellite. *Automatica*, 44(7), 2008.

[21] D Bortoluzzi, P Bosetti, Carbone L, Cavalleri A, Ciccolella A, M Da Lio, K Danzmann, R Dolesi, A Gianolio, G Heinzel, D Hoyland, C D Hoyle, M Hueller, F Nappo, M Sallusti, P Sarra, M Te Platte, C Tirabassi, S Vitale, and W J Weber. Testing LISA drag-free control with the LISA technology package flight experiment. *Classical and Quantum Gravity*, 20(10), 2003.

[22] S. Kawamura, M. Ando, N. Seto, S. Sato, M. Musha, I. Kawano, and et al. Current status of space gravitational wave antenna DECIGO and B-DECIGO. *Progress of Theoretical and Experimental Physics*, (5), 2021.

[23] ScienceDaily. Krypton Hall effect thruster for spacecraft propulsion. October 6, 2011.

[24] satnews. Starlink Satellite Loss Explained. February 13, 2022.

[25] D. Knipp, V. Ray, E. Sutton, and D. Lin. The “Last Hurrah” of Solar Cycle 23 with Lessons for Solar Cycle 25. In *Triennial Earth Sun Summit Meeting, American Astronomical Society*, Bellevue/Seattle, WA, 8-11 August, 2022.

[26] M.F. Storz, B.R. Bowman, M.J.I Branson, S.J. Casali, and W.K. Tobiska. High Accuracy Satellite Drag Model (HASDM). *Advances in Space Research*, 36:2497–2505, 2005.